Controllable synthesis of metal selenide heterostructures mediated by Ag2Se nanocrystals acting as catalysts

ARTICLE *in* NANOSCALE · SEPTEMBER 2013

Impact Factor: 7.39 · DOI: 10.1039/c3nr03601d · Source: PubMed

4 AUTHORS:

Jiangcong Zhou
Chinese Academy of Sciences
9 PUBLICATIONS **40** CITATIONS
SEE PROFILE

Feng Huang
Chinese Academy of Sciences
33 PUBLICATIONS **676** CITATIONS
SEE PROFILE

Ju Xu
Chinese Academy of Sciences
32 PUBLICATIONS **292** CITATIONS
SEE PROFILE

Yuansheng Wang
Chinese Academy of Sciences
159 PUBLICATIONS **4,273** CITATIONS
SEE PROFILE

Nanoscale

RSC Publishing

PAPER

View Article Online
View Journal | View Issue

Controllable synthesis of metal selenide heterostructures mediated by Ag_2Se nanocrystals acting as catalysts†

Cite this: *Nanoscale*, 2013, **5**, 9714

Jiangcong Zhou, Feng Huang,* Ju Xu and Yuansheng Wang*

Ag_2Se nanocrystals were demonstrated to be novel semiconductor mediators, or in other word catalysts, for the growth of semiconductor heterostructures in solution. This is a result of the unique feature of Ag_2Se as a fast ion conductor, allowing foreign cations to dissolve and then to heterogrow the second phase. Using Ag_2Se nanocrystals as catalysts, dimeric metal selenide heterostructures such as Ag_2S_e–CdSe and Ag_2S_e–ZnSe, and even multi-segment heterostructures such as Ag_2S_e–CdS_e–ZnSe and Ag_2S_e–ZnS_e–CdSe, were successfully synthesized. Several interesting features were found in the Ag_2Se based heterogrowth. At the initial stage of heterogrowth, a layer of the second phase forms on the surface of an Ag_2Se nanosphere, with a curved junction interface between the two phases. With further growth of the second phase, the Ag_2Se nanosphere tends to flatten the junction surface by modifying its shape from sphere to hemisphere in order to minimize the conjunct area and thus the interfacial energy. Notably, the crystallographic relationship of the two phases in the heterostructure varies with the lattice parameters of the second phase, in order to reduce the lattice mismatch at the interface. Furthermore, a small lattice mismatch at the interface results in a straight rod-like second phase, while a large lattice mismatch would induce a tortuous product. The reported results may provide a new route for developing novel selenide semiconductor heterostructures which are potentially applicable in optoelectronic, biomedical, photovoltaic and catalytic fields.

Received 13th July 2013
Accepted 12th August 2013

DOI: 10.1039/c3nr03601d

www.rsc.org/nanoscale

Introduction

In the past decade, semiconductor nanoheterostructures have attracted great interest for their abilities to combine diverse functionalities within a single nanostructure and even generate novel properties, which will undoubtedly lead to revolutionary new applications of nanomaterials in various industry fields.[1] Enormous efforts have been devoted to developing effective routes for fabricating nanoheterostructures in solution. To date, three types of synthetic routes are widely used in the literature for creating nanoheterostructures: the partial ion exchange reaction,[2] the seeded hetero-epitaxial growth,[3] and the catalyst-assisted growth.[4] Among them, the catalyst-assisted growth mode exhibits several unique features, such as high tolerance for lattice mismatches between different components of the heterostructure and ease of fabrication of multi-segment 1D nanoheterostrucutres.[4–6]

For catalyst-assisted growth, several preconditions are required:[4b,7a] (1) the initial catalyst particle must have a melting point below the reaction temperature; (2) the solubility of the aim material in the catalyst should be limited; and (3) formation of a solid solution of the catalyst and the aim material is not allowed. At present, the catalysts discovered that meet the above prerequisites are confined to some expensive metals and alloys, such as Au, In, Bi, Al_xGa_{1-x} alloys, and so on.[6a–f]

Recently, Ag_2S and $Cu_{1.94}S$ nanoparticles have been found to be the effective sulfide catalysts for synthesizing some metal sulfide semiconductor heterostructures, such as Ag_2S–CdS, Ag_2S–ZnS, $Cu_{1.94}S$–ZnS and Cu_2S–In_2S_3, following catalyst-assisted growth.[7] Unlike traditional metal catalysts, Ag_2S and $Cu_{1.94}S$ exhibit activities at temperatures below their melting points, which allows mild solution syntheses, due to their unique features as fast ion conductors in which the cations would behave like a "fluid" to generate vacancies for foreign cations to dissolve and heterogrow the second phase.[7a] However, this kind of semiconductor catalyst can only be used to heterogrow the congeneric semiconductors (*i.e.*, metal sulfides), therefore searching other kind of semiconductor catalysts to construct more semiconductor heterostructures with special functions is highly desired.

Ag_2Se is also a fast ion conductor.[8] Herein, Ag_2Se nanoparticles are demonstrated, for the first time, to be a novel selenide catalyst exhibiting high catalytic activity for construction

State Key Laboratory of Structural Chemistry, Fujian Institute of Research on the Structure of Matter, Chinese Academy of Sciences, Fuzhou, Fujian, 350002, P. R. China. E-mail: yswang@fjirsm.ac.cn; fengh@fjirsm.ac.cn

† Electronic supplementary information (ESI) available: Fig. S1–S8 and Table S1. See DOI: 10.1039/c3nr03601d

of dimeric metal selenide heterostructures such as Ag_2Se–CdSe and Ag_2Se–ZnSe, and even multi-segment heterostructures, such as Ag_2Se–CdSe–ZnSe and Ag_2Se–ZnSe–CdSe. It is found that, at the initial stage of heterogrowth, a layer of the second phase forms on the surface of an Ag_2Se nanosphere, with a curved junction interface between the two phases. With further growth of the second phase, the Ag_2Se nanosphere tends to flatten the junction surface by modifying its shape from sphere to hemisphere in order to minimize the conjunct area and thus the interfacial energy. Notably, the crystallographic relationship of the two phases in the heterostructure varies with the lattice parameters of the second phase, in order to reduce the lattice mismatch at the interface. Furthermore, a small lattice mismatch at the interface results in a straight rod-like second phase, while a large lattice mismatch would induce a tortuous product.

Experimental

Materials

$AgNO_3$, selenium powder, cadmium acetate, zinc acetate, cyclohexane, ethanol, and all of the other solvents employed in the current research were commercially available analytical-grade products. Oleylamine (OAm, >98%) was purchased from Aldrich. All reagents were used as received without further purification.

Preparation of organo-selenium precursor

Se–OAm precursor was prepared by mixing 1 mmol selenium powder with 10 mL oleylamine and heating at 230 °C until a clear solution was formed.

Synthesis of Ag_2Se nanocrystals

The synthesis of spherical silver selenide nanocrystals was accomplished *via* direct reaction of $AgNO_3$ and Se–OAm precursors in oleylamine as a solvent. Typically, oleylamine (8 mL) was heated to 120 °C in a flask with bubbling N_2 and kept at this temperature for 20 min with stirring to get rid of water and other volatile impurities in the oleylamine. Then $AgNO_3$ (34 mg) and Se–OAm precursor (2 mL) were added in turn. After the addition of Se–OAm precursor, the color of the reaction mixture changed from straw yellow to jet black, indicating the formation of Ag_2Se nanocrystals. After further reaction for 60 min at 120 °C, the Ag_2Se nanocrystals were precipitated using ethanol, and collected by centrifugation.

Synthesis of Ag_2Se–CdSe and Ag_2Se–ZnSe heterostructures

In a typical synthesis of Ag_2Se–CdSe heterostructures, Ag_2Se nanocrystals (0.1 g) were dissolved in oleylamine (8 mL). After the temperature reached 180 °C, cadmium acetate (133 mg) and Se–OAm precursor (2 mL) were added in turn and reacted for varying times (1 min, 2 min, 4 min, 7 min) at 180 °C. The products were collected by centrifugation and dispersed in cyclohexane for further characterization. The synthesis of Ag_2Se–ZnSe heterostructures was similar to the Ag_2Se–CdSe heterostructures, but cadmium acetate was replaced by zinc acetate.

Synthesis of Ag_2Se–CdSe–ZnSe and Ag_2Se–ZnSe–CdSe heterostructures

The multi-segment heterostructures were prepared using a sequential addition method. In a typical synthesis of Ag_2Se–CdSe–ZnSe heterostructures, Ag_2Se nanocrystals (0.1 g) were dissolved in oleylamine (8 mL). After the temperature reached 180 °C, zinc acetate (50 mg) and Se–OAm precursor (1 mL) were added in turn under stirring and reacted for 5 min at this temperature. Next, cadmium acetate (65 mg) and Se–OAm precursors (1 mL) were added under stirring and reacted for another 5 min at this temperature. Finally, the products were collected by centrifugation and dispersed in cyclohexane for further characterization. The synthesis of Ag_2Se–ZnSe–CdSe heterostructures was similar to that of the Ag_2Se–CdSe–ZnSe heterostructures, but the addition sequence of cadmium acetate and zinc acetate was be changed.

Characterizations

XRD analyses were carried out with a powder diffractometer (DMAX 2500 RIGAKU) using $Cu_{K\alpha}$ radiation (λ = 0.154 nm). TEM observations were performed using a transmission electron microscope (JEM-2010) equipped with an energy dispersive X-ray spectroscope (EDS). TEM specimens were prepared by directly drying a drop of the dilute cyclohexane dispersion solution of the products on the surface of a carbon-coated copper grid.

Results and discussion

The Ag_2Se nanocrystals were synthesized *via* a reaction between $AgNO_3$ and Se–OAm precursors in oleylamine. As revealed by the X-ray diffraction (XRD) pattern shown in Fig. 1a, the products are pure orthorhombic Ag_2Se with a mean size of 8 nm determined by the Scherrer equation. Transmission electron microscopy (TEM) observations indicated that the Ag_2Se products are monodispersed nanospheres, and each particle is a single-crystal, as shown in Fig. 1b.

By injecting the cadmium acetate and Se–OAm precursors into the hot reaction mixture containing Ag_2Se nanocrystals, Ag_2Se–CdSe heterostructures were prepared. As revealed by the XRD pattern presented in Fig. 2b, the product comprises two

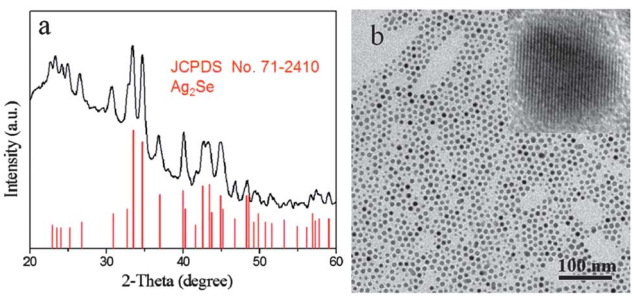

Fig. 1 (a) XRD pattern of the Ag_2Se nanocrystals; the bars on the bottom show the standard data of orthorhombic Ag_2Se (JCPDS no. 71-2410); (b) TEM micrograph of the Ag_2Se nanocrystals; inset in (b) is the HRTEM image of an individual Ag_2Se particle.

phases: the orthorhombic structured Ag_2Se and the hexagonal structured CdSe. The TEM micrograph shown in Fig. 2a reveals that each heterostructure comprises of an Ag_2Se "head" and a CdSe "stick", exhibiting a matchstick morphology. The component of the "head" and the "stick" were confirmed by energy disperse spectroscopy (EDS) spectra recorded at the tip and rod regions respectively (Fig. S1 and S2†).

The HRTEM image and FFT pattern shown in Fig. 3 demonstrate that, for an individual Ag_2Se–CdSe heterostructure, Ag_2Se provides its (002) plane to form the interface with the $(10\bar{1}0)$ plane of CdSe, while the (200) planes of Ag_2Se consecutively connect with the $(1\bar{2}10)$ ones of CdSe at the heterojunction, with the lattice mismatch therein being 0.8%.

The morphological evolution of the Ag_2Se–CdSe nanoheterostructures was monitored by TEM observations, as shown in Fig. 4. After 1 min reaction, a layer of CdSe nanophase appears on the surface of an Ag_2Se nanosphere with distinguishable contrast, forming a dimeric Ag_2Se–CdSe heterostructure (Fig. 4a). Further increasing the reaction time to 2 min, 4 min and 7 min, the CdSe segment grows longer and longer, forming a nanorod with Ag_2Se remaining on the tip (Fig. 4b–d). Remarkably, at the initial stage of CdSe heterogrowth, the interface between the Ag_2Se catalyst and the CdSe layer is curved. With further growth of CdSe, the Ag_2Se "head" tends to modulate its shape from sphere to hemisphere, providing a more flat surface to couple with CdSe in order to reduce the conjunct area and thus the interfacial energy. During such shape modulation, the volume of the Ag_2Se catalyst remains basically unchanged. This shape modulation behavior is enabled by the fluidic feature of Ag ions in Ag_2Se which make the Ag_2Se nanoparticle flexible.[7a,c] Eventually, a clear heterojunction with a defined crystallographic relationship for the two phases is generated. It is worth noting that, in a similar reaction but without Ag_2Se, instead of hexagonal structured CdSe nanorods, cubic structured CdSe nanopyramids were produced (Fig. S3 and S4†), which indicates that Ag_2Se nanocrystals play an important role in determining the phase structure and shape of CdSe.

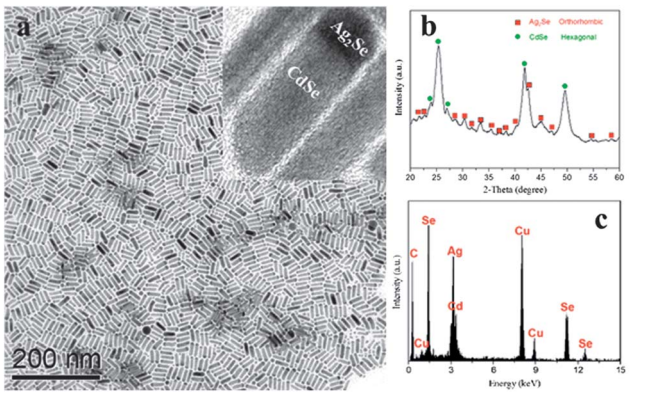

Fig. 2 (a) TEM micrograph of the matchstick-like Ag_2Se–CdSe nanoheterostructures; (b) XRD pattern of the Ag_2Se–CdSe heterostructures; (c) EDS spectrum of the Ag_2Se–CdSe nanoheterostructures, showing the existence of Ag, Cd and Se; the C and Cu signals come from the copper grid; inset in (a) is a HRTEM image of Ag_2Se–CdSe nanoheterostructures.

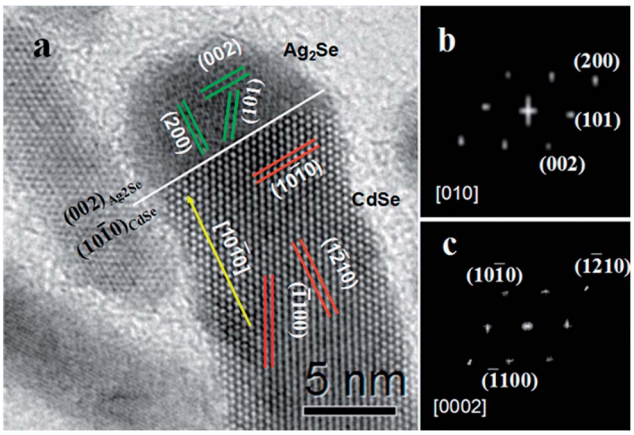

Fig. 3 (a) HRTEM image of an individual Ag_2Se–CdSe nanoheterostructure; (b) and (c) are the fast Fourier transform (FFT) patterns taken from Ag_2Se and CdSe regions respectively.

The formation mechanism of the Ag_2Se–CdSe heterostructure is believed to be the catalyst-assisted growth of CdSe on Ag_2Se, in which the Ag_2Se nanoparticle acts as a catalyst, allowing the Cd ions in solution to dissolve. When the Cd concentration is saturated, they are expelled from the catalyst, forming a CdSe layer on the surface of Ag_2Se which then grows to be a nanorod. A similar mechanism was reported for the formation of metal sulfide heterostructures by Xu *et al.* and Tang *et al.*[7a,c]

Using Ag_2Se nanocrystals as catalyst, Ag_2Se–ZnSe heterostructures were also prepared *via* a co-precipitation reaction. As demonstrated by the TEM, XRD and EDS analyses shown in Fig. 5, the produced heterostructures consist of an Ag_2Se tip and a tortuous ZnSe nanowire. Despite ZnSe having the same

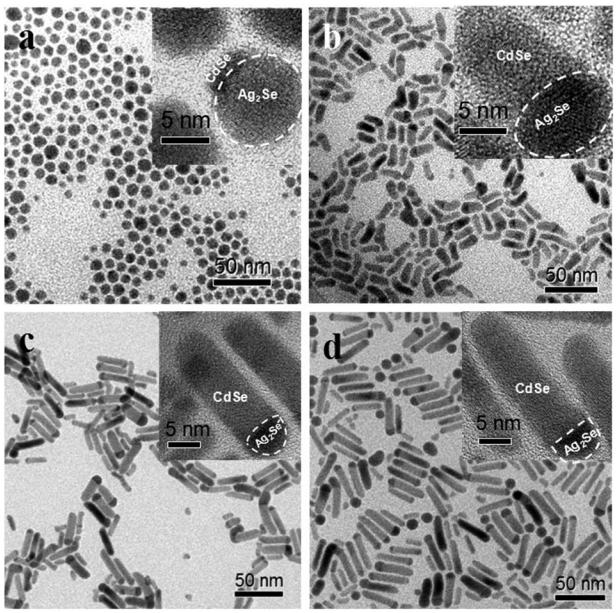

Fig. 4 TEM micrographs of Ag_2Se–CdSe nanoheterostructures having reacted for (a) 1 min, (b) 2 min, (c) 4 min and (d) 7 min, respectively; insets are the corresponding HRTEM images of the nanoheterostructures.

hexagonal structure as CdSe, the HRTEM image and FFT pattern presented in Fig. 6 reveal that, different from the case in the Ag_2Se–CdSe heterostructures, Ag_2Se provides its (012) plane to form the interface with the (0002) plane of ZnSe, while the $(0\bar{2}1)$ planes of Ag_2Se consecutively connect with the $(10\bar{1}0)$ ones of ZnSe at the interface, with the lattice mismatch therein being 6.7% (Fig. S5†). This result indicates that the crystallographic relationship of the two phases in the heterostructure varies with the lattice parameters of the second phase. If the Ag_2Se–ZnSe heterostructure adopted the same crystallographic relationship as that of the Ag_2Se–CdSe one, *i.e.*, Ag_2Se provides its (002) plane to form the interface with the $(10\bar{1}0)$ plane of ZnSe, the lattice mismatch at the interface would be as large as 8.5%, which would result in a high interfacial energy. To reduce the system energy of the heterostructure, a more suitable interface, constructed from $(012)_{Ag_2Se}$ and $(0002)_{ZnSe}$, is therefore generated. However, the 6.7% lattice mismatch is still remarkably larger than that of the Ag_2Se–CdSe heterostructure. During catalyst-assisted growth, such a large lattice mismatch would undoubtedly induce many lattice defects in the ZnSe nanowire, and make it tortuous. As revealed by the HRTEM observation presented in Fig. S6,† the ZnSe nanowire in a tortuous Ag_2Se–ZnSe nanoheterostructure has several turnings, and each turning exhibits the same crystallographic structure, indicating the whole ZnSe nanowire being a single crystal.

To further discuss the key role of lattice mismatch between Ag_2Se and the other selenide in the formation of heterostructures, the calculated lattice mismatches of some possible plane-couplings (heterojunctions) for Ag_2Se and the second phase (ZnSe or CdSe) in present work are listed in Table S1.† Among these possible plane-couplings, the experimentally observed (002) Ag_2Se/$(10\bar{1}0)$ CdSe and (012) Ag_2Se/(0002) ZnSe ones exhibit the smallest lattice mismatches for the Ag_2Se–CdSe and Ag_2Se–ZnSe heterojunctions, respectively, which confirms that the two-phase constructed heterostructures tend to choose the crystallographic relationship with a smallest lattice mismatch between Ag_2Se and the second phase to minimize the interfacial energy.

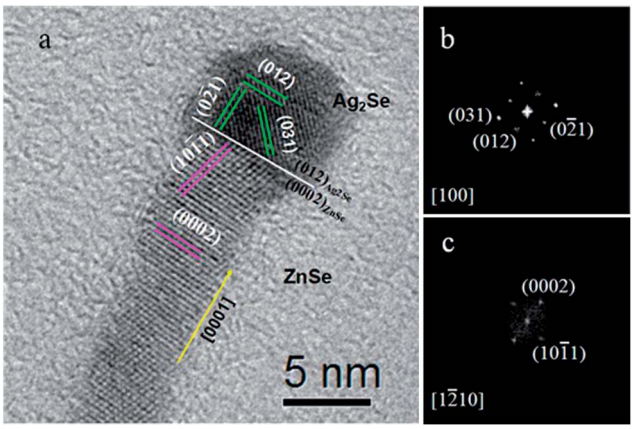

Fig. 6 (a) HRTEM image of an individual Ag_2Se–ZnSe nanoheterostructure; (b) and (c) are the fast Fourier transform (FFT) patterns taken from the Ag_2Se and ZnSe regions respectively.

Following the catalyst-assisted growth mechanism, multi-segment semiconductor heterostructures can be constructed through a sequential addition process, as schematically illustrated in Fig. 7a. After injecting cadmium acetate as the Cd source into the solution containing the pre-preformed Ag_2Se–ZnSe nanoheterostructures, CdSe nanorods are generated between the Ag_2Se head and the ZnSe segment, forming a trimeric Ag_2Se–CdSe–ZnSe semiconductor heterostructure, as shown in Fig. 7b and c (EDS spectra recorded from the different regions of an Ag_2Se–CdSe–ZnSe heterostructure are presented in Fig. S7 and S8†). In such trimeric heterostructures, the crystallographic relationship of Ag_2Se and CdSe is the same as that in the Ag_2Se–CdSe dimeric heterostructure (inset of Fig. 7c), which means that, when the CdSe mid-segment is generated, the Ag_2Se "head" tilts 20° to provide its (002) plane to couple with the $(10\bar{1}0)$ one of CdSe, driven by the tendency to reduce the lattice mismatch and the related interfacial energy of the Ag_2Se–CdSe heterojunction. In other words, during the

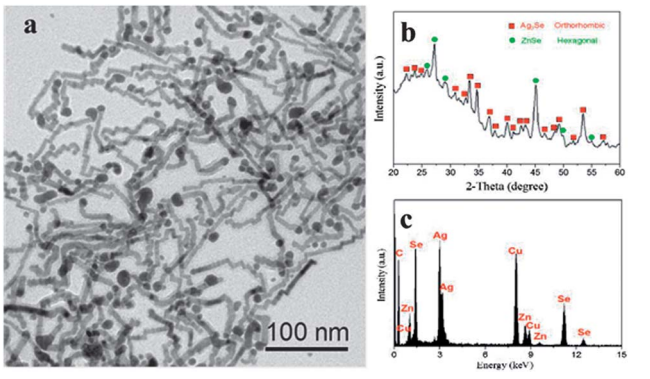

Fig. 5 (a) TEM micrograph of Ag_2Se–ZnSe nanoheterostructures; (b) XRD pattern of Ag_2Se–ZnSe nanoheterostructures; (c) EDS spectrum of Ag_2Se–ZnSe nanoheterostructures showing the existence of Ag, Zn and Se; the C and Cu signals come from the copper grid.

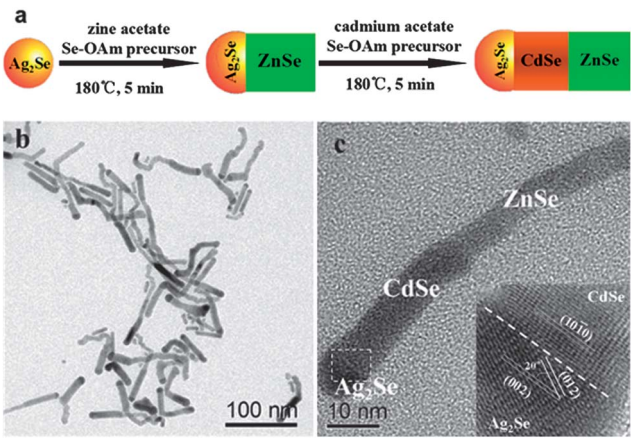

Fig. 7 (a) Schematic illustration of the formation of an Ag_2Se–CdSe–ZnSe nanoheterostructure; (b) TEM micrograph of Ag_2Se–CdSe–ZnSe heterostructures; (c) HRTEM image of an individual Ag_2Se–CdSe–ZnSe heterostructure; inset of (c) is the HRTEM image taken from the frame marked region in (c).

sequential catalyst-assisted growth of a multi-segment heterostructure, the catalyst could modulate its crystallographic orientation and the junction plane to keep the energy of the Ag_2Se-based interface low, therefore benefiting the thermal stability of the multi-segment heterostructure. Using a similar operation but a different order of reactant-addition, Ag_2Se–ZnSe–CdSe heterostructures could also be fabricated, as shown in Fig. 8. Herein, the Ag_2Se catalyst provides its (012) plane to couple with the (0002) one of the ZnSe mid-segment, as demonstrated by the inset of Fig. 8b. Notably, in the sequential catalyst-assisted growth of the multi-segment heterostructure, the third phase always comes between the Ag_2Se catalyst and the second phase, and not on the opposite side of Ag_2Se, which is attributed to the reason that the pre-formed heterojunction between the Ag_2Se catalyst and the second phase, with defects induced by lattice mismatch, provides more active nucleation sites for the growth of the third phase. It is believed that, using Ag_2Se as catalyst, many kinds of technologically important metal selenide heterostructures could be designed and fabricated.

In summary, Ag_2Se nanocrystals were demonstrated to be novel semiconductor mediators, or in other word catalysts, for the growth of metal selenide semiconductor heterostructures in solution, which benefit from the unique feature of Ag_2Se as a fast ion conductor allowing foreign cations to dissolve and then to heterogrow the second phase. Using Ag_2Se nanocrystals as catalysts, dimeric metal selenide heterostructures such as Ag_2Se–CdSe and Ag_2Se–ZnSe, and even multi-segment heterostructures such as Ag_2Se–CdSe–ZnSe and Ag_2Se–ZnSe–CdSe, were successfully synthesized. At the initial stage of the Ag_2Se assisted heterogrowth, a layer of the second phase forms on the surface of Ag_2Se nanosphere, with a curved junction interface between the two phases. With further growth of the second phase, the Ag_2Se nanosphere tends to flatten the junction surface by modifying its shape from sphere to hemisphere in order to minimize the conjunct area and thus the interfacial energy. Notably, the crystallographic relationship of the two phases in the heterostructure varies with the lattice parameters of the second phase, in order to reduce the lattice mismatch at the interface. Furthermore, a small lattice mismatch at the interface results in a straight rod-like second phase, while a large lattice mismatch would induce a tortuous product.

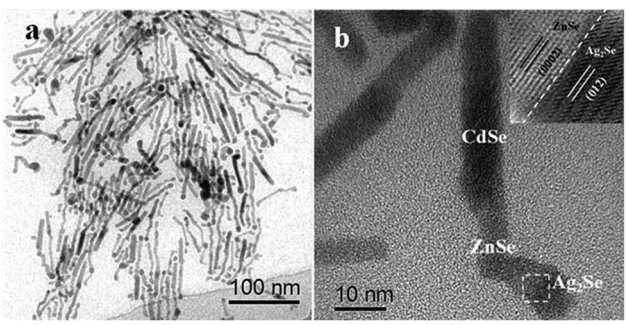

Fig. 8 (a) TEM micrograph of Ag_2Se–ZnSe–CdSe heterostructures; (b) HRTEM image of an Ag_2Se–ZnSe–CdSe heterostructure; inset of (b) is HRTEM image taken from the frame marked region in (b).

Acknowledgements

This work was supported by the National Natural Science Foundation of China (11204301, 21271170, 51202244 and 51172231) and Fund of Key Laboratory of Optoelectronic Materials Chemistry and Physics, Chinese Academy of Sciences (2011KL008).

Notes and references

1 (*a*) D. J. Milliron, S. M. Hughes, Y. Cui, L. Manna, J. B. Li, L. W. Wang and A. P. Alivisatos, *Nature*, 2004, **430**, 190–194; (*b*) L. Ouyang, K. N. Maher, C. L. Yu, J. McCarty and H. Park, *J. Am. Chem. Soc.*, 2007, **129**, 133–138; (*c*) P. T. Chin, C. D. Donega, S. S. Bavel, S. C. J. Meskers, N. A. J. M. Sommerdijk and R. A. J. Janssen, *J. Am. Chem. Soc.*, 2007, **129**, 14880–14886; (*d*) S. H. Choi, H. B. Na, Y. Park, K. An, S. G. Kwon, Y. Jang, M. Park, J. Moon, J. S. Son, I. C. Song, W. K. Moon and T. Hyeon, *J. Am. Chem. Soc.*, 2008, **130**, 15573–15580; (*e*) M. T. Niu, F. Huang, L. F. Cui, P. Huang, Y. L. Yu and Y. S. Wang, *ACS Nano*, 2010, **4**, 681–688; (*f*) P. Li, Z. Wei, T. Wu, Q. Peng and Y. D. Li, *J. Am. Chem. Soc.*, 2011, **133**, 5660–5663; (*g*) L. Wu, B. G. Quan, Y. L. Liu, R. Song and Z. Y. Tang, *ACS Nano*, 2011, **5**, 2224–2230; (*h*) M. B. Cortie and A. M. McDonagh, *Chem. Rev.*, 2011, **111**, 3713–3735; (*i*) J. Johansson and K. A. Dick, *CrystEngComm*, 2011, **13**, 7175–7184; (*j*) E. Cassette, B. Mahler, J. M. Guigner, G. Patriarche, B. Dubertret and T. Pons, *ACS Nano*, 2012, **6**, 6741–6750; (*k*) H. B. Li, R. Brescia, R. Krahne, G. Bertoni, M. J. P. Alcocer, C. Andrea, F. Scotognella, F. Tassone, M. Zanella, M. D. Giorgi and L. Manna, *ACS Nano*, 2012, **6**, 1637–1647; (*l*) J. C. Zhou, F. Huang, J. Xu and Y. S. Wang, *CrystEngComm*, 2013, **15**, 4217–4220.

2 (*a*) R. D. Robinson, B. Sadtler, D. O. Demchenko, C. K. Erdonmez, L. W. Wang and A. P. Alivisatos, *Science*, 2007, **317**, 355–358; (*b*) D. O. Demchenko, R. D. Robinson, B. Sadtler, C. K. Erdonmez, A. P. Alivisatos and L. W. Wang, *ACS Nano*, 2008, **2**, 627–636; (*c*) J. M. Luther, H. M. Zheng, B. Sadtler and A. P. Alivisatos, *J. Am. Chem. Soc.*, 2009, **131**, 16851–16857; (*d*) C. O. Sullivan, R. D. Gunning, A. Sanyal, C. A. Barrett, H. Geaney, F. R. Laffir, S. Ahmed and K. M. Ryan, *J. Am. Chem. Soc.*, 2009, **131**, 12250–12257; (*e*) B. Sadtler, D. O. Demchenko, H. M. Zheng, S. M. Hughes, M. G. Merkle, U. Dahmen, L. W. Wang and A. P. Alivisatos, *J. Am. Chem. Soc.*, 2009, **131**, 5285–5293; (*f*) M. L. Pang, J. Y. Hu and H. C. Zeng, *J. Am. Chem. Soc.*, 2010, **132**, 10771–10785; (*g*) M. Kruszynska, H. Borchert, J. Parisi and J. K. Olesiak, *J. Am. Chem. Soc.*, 2010, **132**, 15976–15986; (*h*) M. D. Regulacio, C. Ye, S. H. Lim, M. Bosman, L. Polavarapu, W. L. Koh, J. Zhang, Q. H. Xu and M. Y. Han, *J. Am. Chem. Soc.*, 2011, **133**, 2052–2055; (*i*) M. Saruyama, Y. G. So, K. Kimoto, S. Taguchi, Y. Kanemitsu and T. Teranishi, *J. Am. Chem. Soc.*, 2011, **133**, 17598–17601; (*j*) S. K. Han, M. Gong, H. B. Yao, Z. M. Wang and S. H. Yu, *Angew. Chem., Int. Ed.*, 2012, **51**, 6365–6368.

3 (*a*) T. Mokari, E. Rothenberg, I. Popov, R. Costi and U. Banin, *Science*, 2004, **304**, 1787–1790; (*b*) P. D. Cozzoli, T. Pellegrino

and L. Manna, *Chem. Soc. Rev.*, 2006, **35**, 1195–1208; (*c*) S. H. Choi, E. G. Kim and T. Hyeon, *J. Am. Chem. Soc.*, 2006, **128**, 2520–2521; (*d*) T. Teranishi, M. Saruyama, M. Nakaya and M. Kanehara, *Angew. Chem., Int. Ed.*, 2007, **46**, 1713–1715; (*e*) T. Teranishi, M. Saruyama and M. Kanehara, *Nanoscale*, 2009, **1**, 225–228; (*f*) L. F. Xi, C. Boothroyd and Y. M. Lam, *Chem. Mater.*, 2009, **21**, 1465–1470; (*g*) J. Yang and J. Y. Ying, *J. Am. Chem. Soc.*, 2010, **132**, 2114–2115; (*h*) W. S. Wang, J. Goebl, L. He, S. Aloni, Y. X. Hu, L. Zhen and Y. D. Yin, *J. Am. Chem. Soc.*, 2010, **132**, 17316–17324; (*i*) F. H. Lin, W. Chen, Y. H. Liao, R. Doong and Y. D. Li, *Nano Res.*, 2010, **3**, 676–684; (*j*) J. Lian, Y. Xu, M. Lin and Y. Chan, *J. Am. Chem. Soc.*, 2012, **134**, 8754–8757; (*k*) M. R. Kim, K. Miszta, M. Povia, R. Brescia, S. Christodoulou, M. Prato, S. Marras and L. Manna, *ACS Nano*, 2012, **6**, 11088–11096; (*l*) P. Rukenstein, H. J. Plante, M. Diab, E. Chockler, K. Flomin, B. Moshofsky and T. Mokari, *CrystEngComm*, 2012, **14**, 7590–7593.

4 (*a*) A. G. Dong, F. D. Wang, T. L. Daulton and W. E. Buhro, *Nano Lett.*, 2007, **7**, 1308–1313; (*b*) D. D. Fanfair and B. A. Korgel, *Cryst. Growth Des.*, 2008, **8**, 3246–3252; (*c*) J. Q. Hu, Y. Bandob and D. Golberg, *J. Mater. Chem.*, 2009, **19**, 330–343; (*d*) S. A. Fortuna and X. L. Li, *Semicond. Sci. Technol.*, 2010, **25**, 024005; (*e*) C. Zou, M. Li, L. J. Zhang, Y. Yang, Q. Li, X. A. Chen, X. J. Xu and S. M. Huang, *CrystEngComm*, 2011, **13**, 3515–3520; (*f*) J. L. Wang, C. M. Yang, Z. P. Huang, M. G. Humphrey, D. Jia, T. T. You, K. M. Chen, Q. Yang and C. Zhang, *J. Mater. Chem.*, 2012, **22**, 10009–10014; (*g*) Z. P. Huang, L. Pan, P. Zhong, M. Y. Li, F. Tian and C. Zhang, *Chem.–Eur. J.*, 2013, **19**, 1732–1739; (*h*) Q. Li, C. Zou, L. L. Zhai, L. J. Zhang, Y. Yang, X. A. Chen and S. M. Huang, *CrystEngComm*, 2013, **15**, 1806–1813.

5 (*a*) S. T. Connor, C. M. Hsu, B. D. Weil, S. Aloni and Y. Cui, *J. Am. Chem. Soc.*, 2009, **131**, 4962–4966; (*b*) J. Y. Chang and C. Y. Cheng, *Chem. Commun.*, 2011, **47**, 9089–9091; (*c*) T. T. Zhuang, F. Fan, M. Gong and S. H. Yu, *Chem. Commun.*, 2012, **48**, 9762–9764; (*d*) F. Huang, J. Xu, D. Q. Chen and Y. Wang, *J. Mater. Chem.*, 2012, **22**, 22614–22618; (*e*) H. B. Shen, H. Y. Shang, J. Z. Niu, W. W. Xu, H. Z. Wang and L. S. Li, *Nanoscale*, 2012, **4**, 6509–6514; (*f*) L. Yi, Y. Liu, N. Yang, Z. Tang, H. Zhao, G. Ma, Z. Su and D. Wang, *Energy Environ. Sci.*, 2013, **6**, 835–840.

6 (*a*) P. D. Markowitz, M. P. Zach, P. C. Gibbons, R. M. Penner and W. E. Buhro, *J. Am. Chem. Soc.*, 2001, **123**, 4502–4511; (*b*) H. Yu, J. Li, R. A. Loomis, L. W. Wang and W. E. Buhro, *Nat. Mater.*, 2003, **2**, 517–520; (*c*) F. Wang, A. Dong, J. Sun, R. Tang, H. Yu and W. E. Buhro, *Inorg. Chem.*, 2006, **45**, 7511–7521; (*d*) J. Puthussery, A. Lan, T. H. Kosel and M. Kuno, *ACS Nano*, 2008, **2**, 357–367; (*e*) A. T. Heitsch, C. M. Hessel, V. A. Akhavan and B. A. Korgel, *Nano Lett.*, 2009, **9**, 3042–3047; (*f*) A. M. Chockla and B. A. Korgel, *J. Mater. Chem.*, 2009, **19**, 996–1001; (*g*) G. Aksomaityte, F. Cheng, A. L. Hector, J. R. Hyde, W. Levason, G. Reid, D. C. Smith, J. W. Wilson and W. Zhang, *Chem. Mater.*, 2010, **22**, 4246–4253.

7 (*a*) W. Han, L. Yi, N. Zhao, A. Tang, M. Y. Gao and Z. Y. Tang, *J. Am. Chem. Soc.*, 2008, **130**, 13152–13161; (*b*) L. X. Yi, A. W. Tang, M. Niu, W. Han, Y. B. Hou and M. Y. Gao, *CrystEngComm*, 2010, **12**, 4124–4130; (*c*) G. X. Zhu and Z. Xu, *J. Am. Chem. Soc.*, 2011, **133**, 148–157; (*d*) S. L. Shen, Y. J. Zhang, L. Peng, Y. P. Du and Q. B. Wang, *Angew. Chem., Int. Ed.*, 2011, **50**, 7115–7118; (*e*) Y. Liang, Y. Tao and S. K. Hark, *CrystEngComm*, 2011, **13**, 5751–5754; (*f*) S. L. Shen, Y. J. Zhang, Y. S. Liu, L. Peng, X. Y. Chen and Q. B. Wang, *Chem. Mater.*, 2012, **24**, 2407–2413; (*g*) F. Huang, J. Xu, D. Q. Chen and Y. Wang, *Nanotechnology*, 2012, **23**, 425604.

8 (*a*) D. T. Schoen, C. Xie and Y. Cui, *J. Am. Chem. Soc.*, 2007, **129**, 4116–4117; (*b*) A. Sahu, L. Qi, M. S. Kang, D. Deng and D. J. Norris, *J. Am. Chem. Soc.*, 2011, **133**, 6509–6512.